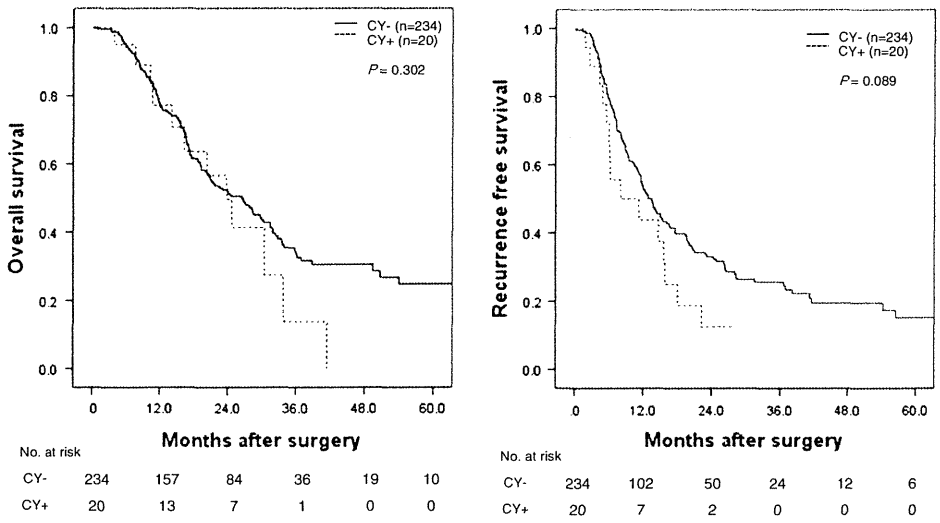

Fig. 1 Overall and recurrence-free survival of patients with negative (CY-) or positive (CY+) peritoneal lavage cytology following pancreatic resection. The median overall survival of CY+ patients and CY- patients was 23.8 (95 % CI, 17.6–29.8) months and 26.5 (95 % CI, 20.7-32.3) months, respectively ($P = 0.302$). The median recurrence-free survival of CY+ and CY- patients was 8.1 (95 % CI, 0.0–17.9) months and 13.5 (95 % CI, 11.5–15.5) months, respectively ($P = 0.089$)

Table 4 The first recurrence site after operation

	CY− *n* (%)	CY+ *n* (%)	*P*
Liver	67 (28)	6 (30)	1.000
Local	29 (12)	3 (15)	0.745
Lymph node	18 (8)	2 (10)	0.675
Lung	23 (10)	0 (0)	0.232
Peritoneum	16 (7)	7 (35)	0.001*
Other	15 (6)	1 (5)	

CY+ positive peritoneal lavage cytology

* Statistically significant

cancer without distant metastases remains controversial. To our knowledge, there is no report that compares the prognosis between resected CY+ patients and unresected CY+ patients without other distant metastasis. The same limitation is equally true of the present study.

Generally, patients with metastatic disease have a short median survival of 3–6 months [2], and FOLFIRINOX, the most promising treatment regimen at present, increased that time to only 11.1 months [20]. Patients with locally advanced nonmetastatic disease have a median survival of 6–10 months without resection, while those who undergo neoadjuvant therapy followed by R0 resection have an overall survival of 20 months [2, 21]. At present, surgical resection remains the only potentially curative treatment for pancreatic cancer, indicating that the median overall survival of 23.8 months in the CY+ patients who underwent resection in the present study was a promising result.

In the present study, CY+ patients showed a higher number of peritoneal recurrences with R1 resection, and the median RFS was shorter in CY+ patients than in CY− patients (8.1 vs. 13.5 months), although the difference was not statistically significant ($P = 0.089$). This insignificant difference might be due to the small number of cases from a single institution and/or the short follow-up period of 24.7 months in the present study.

Table 5 Published studies analyzing the correlation between survival and CY status in patients who underwent resection

Author	Journal	Year		*n*	Median survival (months)	*P* value
Yachida et al. [15]	Br J Surg	2002	CY−	114	NA	0.347
			CY+	16	NA	
Meszoely et al. [12]	Am Surg	2004	CY−	122	19	0.055
			CY+	13	15	
Ferrone et al. [19]	J Gastrointest Surg	2006	CY−	207	16	<0.001
			CY+	10	8	
Yamada et al. [16]	Ann Surg	2007	CY−	136	13.5	0.269
			CY+	21	13.6	
Present study		2011	CY−	234	26.5	0.302
			CY+	20	23.8	

NA not available, *CY+* positive peritoneal lavage cytology

In conclusion, positive peritoneal lavage cytology was not associated with overall survival after resection, despite of the increased frequency of peritoneal recurrence. CY+ status without other distant metastasis does not necessarily preclude resection in patients with pancreatic cancer.

Acknowledgments This study was supported by a grant-in-aid for cancer research from the Ministry of Health, Welfare and Labor of Japan and by the Japanese Foundation for Promotion of Cancer Research.

Conflict of interest The authors declare no personal conflict of interest and no financial support for the study.

References

1. Siegel R, Ward E, Brawley O, Jemal A (2011) Cancer statistics, 2011: the impact of eliminating socioeconomic and racial disparities on premature cancer deaths. CA Cancer J Clin 61: 212–236
2. Gillen S, Schuster T, Meyer Zum Buschenfelde C et al (2010) Preoperative/neoadjuvant therapy in pancreatic cancer: a systematic review and meta-analysis of response and resection percentages. PLoS Med 7:e1000267
3. Aletti GD, Gallenberg MM, Cliby WA et al (2007) Current management strategies for ovarian cancer. Mayo Clin Proc 82:751–770
4. Japanese Gastric Cancer Association (2011) Japanese classification of gastric carcinoma: 3rd English edition. Gastric Cancer 14:101–112
5. American Joint Committee on Cancer (2010) Exocrine and endocrine pancreas. In: The AJCC Cancer Staging Manual, 7th ed. Springer, New York, pp 241–249
6. Clark CJ, Traverso LW (2010) Positive peritoneal lavage cytology is a predictor of worse survival in locally advanced pancreatic cancer. Am J Surg 199:657–662
7. Fernandez-del Castillo C, Rattner DW, Warshaw AL (1995) Further experience with laparoscopy and peritoneal cytology in the staging of pancreatic cancer. Br J Surg 82:1127–1129
8. Jimenez RE, Warshaw AL, Fernandez-Del Castillo C (2000) Laparoscopy and peritoneal cytology in the staging of pancreatic cancer. J Hepatobiliary Pancreat Surg 7:15–20
9. Leach SD, Rose JA, Lowy AM et al (1995) Significance of peritoneal cytology in patients with potentially resectable adenocarcinoma of the pancreatic head. Surgery 118:472–478
10. Makary MA, Warshaw AL, Centeno BA et al (1998) Implications of peritoneal cytology for pancreatic cancer management. Arch Surg 133:361–365
11. Merchant NB, Conlon KC, Saigo P et al (1999) Positive peritoneal cytology predicts unresectability of pancreatic adenocarcinoma. J Am Coll Surg 188:421–426
12. Meszoely IM, Lee JS, Watson JC et al (2004) Peritoneal cytology in patients with potentially resectable adenocarcinoma of the pancreas. Am Surg 70:208–213 discussion 213–204
13. Nakao A, Fujii T, Sugimoto H et al (2006) Oncological problems in pancreatic cancer surgery. World J Gastroenterol 12: 4466–4472
14. Warshaw AL (1991) Implications of peritoneal cytology for staging of early pancreatic cancer. Am J Surg 161:26–29 discussion 29–30
15. Yachida S, Fukushima N, Sakamoto M et al (2002) Implications of peritoneal washing cytology in patients with potentially resectable pancreatic cancer. Br J Surg 89:573–578
16. Yamada S, Takeda S, Fujii T et al (2007) Clinical implications of peritoneal cytology in potentially resectable pancreatic cancer: positive peritoneal cytology may not confer an adverse prognosis. Ann Surg 246:254–258
17. Ueno H, Kosuge T, Matsuyama Y et al (2009) A randomised phase III trial comparing gemcitabine with surgery-only in patients with resected pancreatic cancer: Japanese Study Group of Adjuvant Therapy for Pancreatic Cancer. Br J Cancer 101:908–915
18. Tempero MA, Arnoletti JP, Behrman S et al (2010) Pancreatic adenocarcinoma. J Natl Compr Cancer Netw 8:972–1017
19. Ferrone CR, Haas B, Tang L et al (2006) The influence of positive peritoneal cytology on survival in patients with pancreatic adenocarcinoma. J Gastrointest Surg 10:1347–1353
20. Conroy T, Desseigne F, Ychou M et al (2011) FOLFIRINOX versus gemcitabine for metastatic pancreatic cancer. N Engl J Med 364:1817–1825
21. Katz MH, Pisters PW, Evans DB et al (2008) Borderline resectable pancreatic cancer: the importance of this emerging stage of disease. J Am Coll Surg 206:833–846 discussion 846–838

Surgical Technique

Importance of Maintaining Left Gastric Arterial Flow at Appleby Operation Preserving Whole Stomach for Central Pancreatic Cancer

Akifumi Kimura[1], Junji Yamamoto[1], Suefumi Aosasa[3], Kazuo Hatsuse[1], Makoto Nishikawa[1], Kiyoshi Nishiyama[1], Hironori Tsujimoto[1], Tomoyuki Moriya[1], Kazuo Hase[1], Hiroshi Shinmoto[2] and Tatsumi Kaji[2]

[1]Department of Surgery and [2]Department of Radiology, National Defense Medical College, Saitama, Japan
[3]Department of Surgery, Social Health Insurance OMIYA General Hospital, Saitama, Japan

Corresponding author: Akifumi Kimura, Department of Surgery, National Defense Medical College, 359-8513, Namiki 3-2, Tokorozawa, Saitama, Japan; E-mail: akifumi@muse.ocn.ne.jp

Key Words: Appleby operation; Pancreatic cancer; Left gastric artery; Celiac axis.

Abbreviations: Three Dimensional (3D); Celiac Axis (CA); Common Hepatic Artery (CHA); Computed Tomography (CT); Distal Pancreatectomy with Celiac Axis Resection (DP-CAR); Gastroduodenal Artery (GDA); Hounsfield Unit (HU); Left Gastric Artery (LGA); Superior Mesenteric Artery (SMA); Splenic Artery (SPA); Quality of Life (QOL).

SUMMARY

The safety of whole stomach-preserving Appleby operation with resection of the left gastric artery (LGA) for pancreatic cancer cannot be assured. The anatomy of the celiac axis (CA) with special regard to the position of the origin of the LGA was examined. Using 3D images of the vascular architecture reconstructed from volume data of helical CT, the length of the CA and the position of the origin of the LGA from the CA were measured in 53 patients. Among 53 patients, 47 patients (89%) had classical anatomy of the CA branches. The mean length (±standard deviation) of the CA and the distance from the root of the LGA to the bifurcation of the CA were 25.2mm (±4.9) (range 14.6-36.5) and 10.3mm (±4.5) (range 2.4-21.9), respectively. In 23 (45%) cases, the LGA arose farther than 10mm away from the bifurcation of the CA. Among six patients with anatomical variation of the arteries, two (4%) had the LGA directly arising from the aorta. Conservation of the LGA at modified Appleby operation would give complete cancer removal by *en bloc* resection of the nerve plexus, without risk of ischemic complications of the stomach and liver.

INTRODUCTION

According to the TNM atlas of the UICC (1), the body of the pancreas is assigned to the parenchyma between the left border of the portal vein and the aorta. This part is astride the important part of the abdominal aorta from which the celiac axis (CA) and superior mesenteric artery (SMA) arise. As a result of such anatomical features and its invasive biological propensity (2), cancer of the body of the pancreas often involves major arterial structures, including the celiac axis (CA) and superior mesenteric artery (SMA), thus being found as unresectable T4 carcinoma (3).

In 1953, the Canadian surgeon Appleby firstly presented a collective report about the feasibility and safety of resection of the CA and CHA with total gastrectomy and distal pancreatectomy for gastric cancer with bulky lymph node metastases around these vessels (4). Nimura *et al.* first adopted Appleby's operation preserving the whole stomach in a patient with T4 pancreatic body carcinoma invading the CA (5) and several authors have reported this procedure (6-10).

Hirano *et al.* (7) reported an excellent outcome of locally advanced central pancreatic carcinoma in the largest series of patients who had undergone such operation, which they named DP-CAR (distal pancreatectomy with celiac axis resection). According to their results, this operation could be safely performed with no mortality. However, postoperative morbidity was high (48%), among which ischemic gastritis was found in 13% of patients. We herein evaluate the anatomy of celiac axis by CT reconstructed angiography and present three patients who underwent Appleby operation preserving the whole stomach with the left gastric artery for cancer of the body of the pancreas and discuss the feasibility and safety of this procedure.

SURGICAL TECHNIQUE

Evaluation of anatomy of celiac axis by CT reconstructed angiography

The anatomy of the CA was analyzed in 53 patients who underwent helical CT for preoperative evaluation of hepatobiliary disease (bile duct cancer (n=29), gallbladder cancer (n=14) and cancer of the papilla of Vater (n=10)) which did not invade near the CA, SMA and their branches. CT images were acquired using two 64-channel multidetector scanners (Aquillion 64™; Toshiba Medical System, Tokyo, Japan) at our hospital. A total of 1.8mL of non-ionic contrast material (iopamidol (300-370mg iodine per mL)) per kilogram body weight was injected into an antecubital vein at a rate of 4.0mL/sec using a power injector. Bolus tracking was used to assure appropriate imaging timing and early and late arterial-phase imaging was performed 5 and 22 seconds after the contrast density in the abdominal aorta reached a predefined threshold of 120 Hounsfield units (HU). From the obtained volume data, 3D images of the vascular architecture, which could be rotated in any direction, were reconstructed. Using these 3D images, the length of the CA and the position of the origin of the LGA from the CA were measured (**Figure 1**).

Hepato-Gastroenterology 2012; 59:2650-2652 doi 10.5754/hge12164

RESULTS

Among 53 patients, six had anatomical variation of the arteries; two had the LGA directly arising from the aorta, two had the splenic artery (SPA) arising before the LGA from the CA and the remaining two had the SPA and the CHA arising from the SMA, respectively. The remaining 47 patients who had classical anatomy of the CA branches were analyzed. The mean length (±standard deviation) of the CA and the distance from the root of the LGA to the bifurcated end of the CA were 25.2mm (±4.9) (range 14.6-36.5) and 10.3mm (±4.5) (range 2.4-21.9), respectively. In 23 (45%) cases, the LGA arose more than 10mm from the bifurcated end of the CA. The longer the CA, the farther the LGA from the bifurcation of the CA ($p<0.05$).

Three patterns of modified Appleby operation (Table 1)

From August 2010 to January 2011, three patients underwent Appleby operation preserving the whole stomach with LGA. All of these cases had advanced pancreatic body cancer without dissemination or distant metastasis and had been suspected tumor invading around the neural plexus of the CA, CHA, or LGA. The details of each patient are shown in **Table 1** and **Figure 2**. Patient 1 had the LGA separately originating from the aorta; thus, the CA was severed at the origin of the aorta. Patient 2 had ordinary vascular anatomy, and the CA was severed distal to the LGA branching. Patient 3 had reconstruction of the LGA with the right inferior phrenic artery after extirpation of the CA at its origin. Postoperative liver dysfunction was mild, with a maximum level of aspartate transaminase of 380IU/L (normal range 9-38 IU/L) in patient 2. The nutritional state of all three patients was good, with percent body weight loss of 0%, 1% and 6% at the last follow-up, respectively. Resection of the CHA and CA was necessary for complete removal of the tumor in all patients.

DISCUSSION

In 1953, Appleby first, and with foresight, presented a collective case series proving that resection of the distal pancreas and total stomach with extirpation of the entire celiac axis and its branches with all of its attendant tissues could be performed with impunity in block dissection for gastric carcinoma. In this operation, hepatopetal arterial flow could be preserved through a double arcade of arterial network surrounding the pancreatic head anteriorly and posteriorly (4). After Nimura *et al.* first succeeded in resecting a central pancreatic carcinoma invading the CA using a similar procedure in which the whole stomach was preserved (5), several authors reported the same operative procedure with various names (6-8,10,13). A total of 48 cases of such operations for central to left-sided pancreatic carcinoma have been reported to date.

Stomach-preserving Appleby operation has been conducted with zero mortality but with high morbidity (7,14). Ischemia of the stomach or the liver is an occasional cause of such complications. In their detailed report, Kondo *et al.* (14) emphasized the uncommonness of ischemic gastropathy after stomach-preserving Appleby's operation except when additional arteries supplying the stomach were divided. However, according to Eleisi *et al.* (15), the arterial blood supply of the stomach is about 60% from the LGA, about 20% from the splenic artery and only about 15% from the right gastric and right gastroepiploic arteries. About 80% of additional replenishing blood flow from the right-side gastric arteries might reduce hepatopetal blood supply through the pancreatic arcades from the SMA; thus, the safety of such procedure for the remnant stomach cannot be assured. Conservation of left gastric arterial flow would help boost arterial irrigation to the liver, thus alleviating both gastric and hepatic ischemia. Postoperative liver ischemia was mild in the present series, the maximum serum value of aspartate aminotransferase being ten times the maximum normal value.

Appleby operation preserving the whole stomach with LGA is indicated for tumors: 1) confined to the neck, body and tail of the pancreas; 2) not invading beyond the bifurcation of the proper hepatic artery and gastroduodenal artery; and 3) not invading the stomach and SMA. There

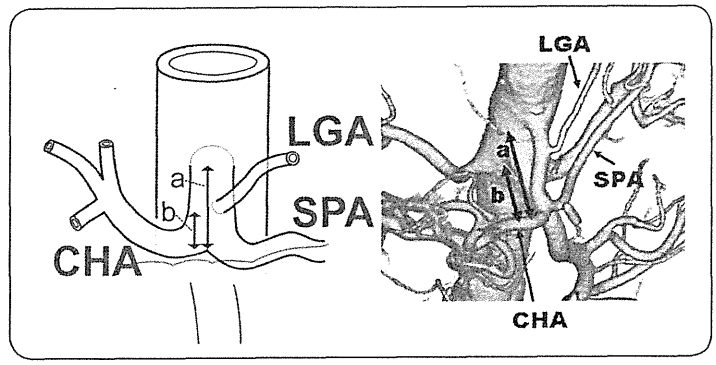

FIGURE 1. Measurement of celiac axis. Using 3D images of the vessel, the length of the celiac axis and the position of the origin of the left gastric artery of the celiac axis were measured. Length (a) is the distance between the root and the end of the celiac axis. Length (b) is the distance from the left gastric artery to the bifurcation of the celiac axis. CHA: Common Hepatic Artery; LGA: Left Gastric Artery; SPA: Splenic Artery.

TABLE 1. Demographic and clinicopathologic data of patients who underwent modified Appleby operation preserving whole stomach with left gastric artery

	Case 1	Case 2	Case 3
Age; Gender	75; F	66; M	60; F
Diagnostic sign	Elevation of CA19-9	Elevation of CA19-9	Appetite loss
Preop CA19-9 (IU/mL)	196.3	4265	1300
Blood loss/op. time	185g/306min	410g/427min	173g/477min
Peak postop. AST*	84	380	135
Complication	Grade B	Grade B	Grade B
Per os start	6 POD	7 POD	6 POD
Time to discharge	30 POD	31 POD	95 POD
Recurrence	None	None	Liver metastasis
Present status	Alive 15 months	Alive 13 months	Alive 9 months
% Weight loss¶	0	1	6
Max. tumor size	23mm	45mm	30mm
Invaded artery	Splenic artery	None	Splenic artery
Invaded vein	Splenic vein	Splenic vein (occlusion) Portal vein	none
(Peri) neural invasion	Celiac axis Splenic artery	Splenic artery	Common hepatic artery Splenic artery
Positive lymph nodes Number of positive nodes/all harvested nodes	Superior peripancreatic 1/27	Superior peripancreatic 9/45	Superior peripancreatic 8/30
Surgical margin	Negative	Negative	Negative

*Normal range of AST (aspartate aminotransferase) is 9 to 38IU/L; ¶Body weight of each patient was measured at the last follow-up.

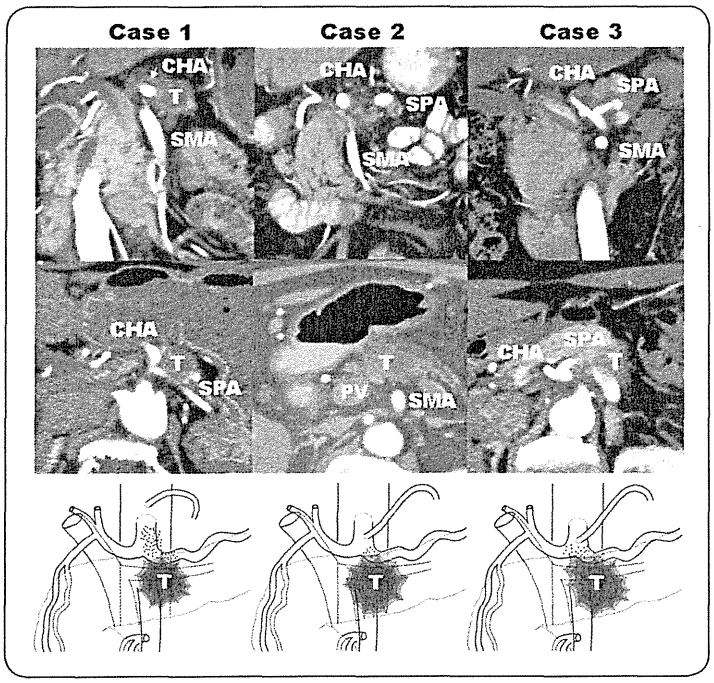

FIGURE 2. Preoperative image and schema of tumor location and its extent of invasion. Three cases of preoperative coronal (upper column) and axial (middle column) image and schema of tumor location and arteries of upper abdomen (lower column) are shown. The dots represent the invasion of the tumors. Each case was suspected tumor invaded around the CA. T: Tumor; CA: Celiac Axis; SPA: Splenic Artery; CHA: Common Hepatic Artery; SMA: Superior Mesenteric Artery.

are several ways to preserve the left gastric arterial flow in stomach-preserving Appleby operation. This operation is most frequently used for a central pancreatic carcinoma, invading or closely approaching the CHA or bifurcation of the CA. Analysis of 3D reconstructed arteriographic images showed an extra surgical margin of 1cm with the LGA-preserving procedure, compared to ordinary distal pancreatectomy. In case of a variation of the LGA directly arising from the aorta (4% of cases), the LGA can be preserved with extirpation of the CA at its origin from the aorta.

As the anatomies of three cases of Appleby operations preserving the whole stomach with the LGA were compatible with those of CT reconstructed angiography respectively, we could estimate the transecting region of artery and the need for reconstruction of the LGA until the operation. These cases have been reported herein, pertaining to the feasibility, safety and effectiveness of this operation. All three patients were alive with good QOL and two of them had no sign of recurrence 15 and 13 months after surgery, respectively. Pathological assessment of the extension of carcinomas in this series showed the presence of cancer cells in the nerve plexus at the root of the SPA. Thus, *en bloc* resection of the nerve plexus with the bifurcated ends of the CA was necessary for complete removal of cancer invasion. Complication-free and QOL-preserving surgery with prompt postoperative adjuvant chemotherapy would be a rational strategy for pancreatic carcinoma.

REFERENCES

1. **Wittekind C, Greene FL, Hutter RVP, et al.:** TNM Atlas (5th ed). Springer; 2004.
2. **Nakao A, Harada A, Nonami T, Kaneko T, Takagi H:** Clinical significance of carcinoma invasion of the extrapancreatic nerve plexus in pancreatic cancer. Pancreas 1996; 12(4):357-361.
3. **Sobin LH, MK G, Ch W:** TNM Classification of malignant tumours (7th ed.), 2009.
4. **Appleby LH:** The coeliac axis in the expansion of the operation for gastric carcinoma. Cancer 1953; 6(4):704-707.
5. **Mayumi T, Nimura Y, Kamiya J, et al.:** Distal pancreatectomy with en bloc resection of the celiac artery for carcinoma of the body and tail of the pancreas. Int J Pancreatol 1997; 22(1):15-21.
6. **Liu B:** Modified Appleby operation in treatment of distal pancreatic cancer. Hepatobiliary Pancreat Dis Int 2003; 2(4):622-625.
7. **Hirano S, Kondo S, Hara T, et al.:** Distal pancreatectomy with en bloc celiac axis resection for locally advanced pancreatic body cancer: long-term results. Ann Surg 2007; 246(1):46-51.
8. **Hishinuma S, Ogata Y, Tomikawa M, Ozawa I:** Stomach-preserving distal pancreatectomy with combined resection of the celiac artery: radical procedure for locally advanced cancer of the pancreatic body. J Gastrointest Surg 2007; 11(6):743-749.
9. **Morera-Ocon FJ, Carcel-Carcel I, Ballestin Vicente J, et al.:** Some reflexions on the modified Appleby procedure. JOP 2009; 10(6):674-678.
10. **Wu X, Tao R, Chongpeng P:** Distal pancreatectomy combined with celiac axis resection: an alternative approach for some advanced diatal pancreatic cancer. Ann Surg Oncol 2010; 17:1359-1366.
11. **Kosuge T, Makuuchi M, Takayama T, et al.:** Thickening at the root of the superior mesenteric artery on sonography: evidence of vascular involvement in patients with cancer of the pancreas. AJR Am J Roentgenol 1991; 156(1):69-72.
12. **Strasberg SM, Drebin JA, Linehan D:** Radical antegrade modular pancreatosplenectomy. Surgery 2003; 133(5):521-527.
13. **Kondo S, Katoh H, Hirano S, et al.:** Results of radical distal pancreatectomy with en bloc resection of the celiac artery for locally advanced cancer of the pancreatic body. Langenbecks Arch Surg 2003; 388(2):101-106.
14. **Kondo S, Katoh H, Hirano S, et al.:** Ischemic gastropathy after distal pancreatectomy with celiac axis resection. Surg Today 2004; 34(4):337-340.
15. **El-Eishi HI, Ayoub SF, El-Khalek MA:** The arterial supply of the human stomach. Acta Anat (Basel) 1973; 86(3):565-580.

Clin Exp Metastasis (2012) 29:101–110
DOI 10.1007/s10585-011-9433-5

RESEARCH PAPER

CXCR4/CXCL12 expression profile is associated with tumor microenvironment and clinical outcome of liver metastases of colorectal cancer

Nozomu Sakai · Hiroyuki Yoshidome · Takashi Shida · Fumio Kimura · Hiroaki Shimizu · Masayuki Ohtsuka · Dan Takeuchi · Masahiro Sakakibara · Masaru Miyazaki

Received: 6 December 2010 / Accepted: 1 November 2011 / Published online: 11 November 2011

Abstract Interaction between CXCR4 and CXCL12 plays a role in tumor progression. The present study examined CXCR4, CXCL12 and CD133 expression in liver metastases of colorectal cancer (CLM) and determined whether the expression profiles affect the tumor microenvironment and thus progression, and whether they could serve as a prognostic marker for survival. Liver metastases of colorectal cancer collected from 92 patients were evaluated by CXCR4, CXCL12 and CD133 immunohistochemistry and clinicopathological data were analyzed. The expression profile of CXCR4 was determined in the colorectal cancer cell line, SW48. The expression of cytoplasmic CXCR4 was higher in 36 (39%) patients than that indicated by CXCR4 staining intensity of hepatocytes. High levels of nuclear CXCR4 expression in 23 (25%) patients significantly correlated with CXCL12 expression in hepatocytes. Nuclear CXCR4 expression was increased in the cancer cells after exposure to CXCL12. Univariate and multivariate analyses demonstrated that the high levels of nuclear CXCR4 and CXCL12 expression in hepatocytes were significantly better prognostic factors for overall and hepatic disease-free survival in patients with CLM. The expression of CXCR4 and CXCL12 in CLM may have an interactive effect that could alter the tumor microenvironment. CXCR4 expression in metastatic liver tumors together with the upregulation of CXCL12 in hepatocytes may help to predict the clinical outcomes of patients with CLM after hepatectomy.

Keywords Colorectal metastases · Hepatectomy · Chemokine · Angiogenesis · CD133

Abbreviations

CLM	Liver metastases of colorectal cancer
EGFR	Epidermal growth factor receptor
EMT	Epithelial-to-mesenchymal transition
FC	Fibrous pseudocapsule

Introduction

Colorectal carcinoma is a leading cause of cancer-related death. Regardless of curative resection to treat colorectal carcinoma, distant metastases develop in a significant number of patients [1]. The liver is a metastatic site of colorectal carcinoma, which is often associated with a poor prognosis [2, 3]. The "seed and soil theory" has been postulated to explain the directional migration and invasion of cancer cells into specific organs [4]. The chemokine network might play a role in the induction of organ-specific metastases [5]. Chemokines and their receptors were originally identified as chemoattractive interactions between immune cells and sites of inflammation [6]. Cancer cells also use chemokine networks to modulate the host microenvironment and facilitate cancer progression [7–10]. Several chemokine receptors and ligands function in tumor progression and invasiveness in several malignancies [11–15]. CXCR4 is an established inducer of colorectal cancer progression that correlates with clinical outcomes of

Nozomu Sakai and Hiroyuki Yoshidome contributed equally to this study.

N. Sakai · H. Yoshidome (✉) · T. Shida · F. Kimura · H. Shimizu · M. Ohtsuka · D. Takeuchi · M. Sakakibara · M. Miyazaki
Department of General Surgery, Chiba University Graduate School of Medicine, 1-8-1 Inohana, Chuo-ku, Chiba 260-8670, Japan
e-mail: h-yoshidome@umin.ac.jp

stage III/IV disease defined by the UICC classification [13]. The CXCR4 ligand, CXCL12/stromal-derived factor-1 (SDF-1), is also associated with tumor progression [16]. Kim et al. found significantly higher CXCR4 expression in liver metastases than in primary colorectal cancer, indicating that CXCL12 is abundantly expressed at metastatic sites [17]. In addition, CXCL12 accumulates in CD133-positive tumor cells that might in part, be derived from cancer stem cells [18, 19]. Therefore, interaction between CXCR4 and CXCL12 expression might cause tumor proliferation, migration, and invasion.

Chemokine receptors generally appear in the cell membrane and cytoplasm, thus leading to downstream signal transduction. CXCR4 is expressed in both the cytoplasm and nucleus of tumor cells [20, 21]. The cytoplasmic expression of CXCR4 is associated with a poor clinical outcome [12], but the nuclear expression of CXCR4 has not been fully elucidated. Furthermore, CXCR4 expression might be altered by the tumor microenvironment [8, 11, 22]. We postulated that different CXCR4/CXCL12 expression profiles in tumor cells and the tumor microenvironment interact and affect each other, thus determining the progression of colorectal liver metastases. In addition, other reports have described that the timing and numbers of liver metastases, lymph node metastasis of the primary tumor, hilar lymph node metastasis and the absence of a fibrous capsule on the metastatic tumor are prognostic factors for survival [23–25]. However, a correlation between the CXCR4/CXCL12 expression and the clinicopathological features of colorectal liver metastases has not been fully elucidated.

The present study examines CXCR4/CXCL12 expression in CLM to determine whether their expression profiles influence the progression of CLM, survival rates and hepatic recurrence.

Patients and methods

Patients and tissue samples

We retrospectively reviewed the medical records of 92 Japanese patients with CLM from among those who underwent curative hepatic resection (R0) at the Department of General Surgery at Chiba University (Chiba, Japan) between 1999 and 2007. Written informed consent was obtained from all of the patients to review their records in accordance with the ethical standards of the Helsinki Declaration of 1975. We defined synchronous metastases as those diagnosed before, or at the time of colorectal surgery. The patients were followed until death or November 30, 2010. The median follow-up time was 38 months (range 8–115 months). The clinicopathological characteristics of the patients are shown in Table 1.

Hematoxylin and eosin (HE) staining and immunohistochemistry

Tissue sections (4 μm thick) prepared from formalin-fixed paraffin-embedded tissue blocks were stained with HE and immunohistochemically assessed using either the CSA II kit for CXCR4 and CD133 or the ENVISION+ kit for CXCL12/SDF-1 (DAKO Cytomation, Carpinteria, CA, USA) according to the manufacturer's instructions. Antigens in all analyses were retrieved by microwave heating. The series and dilutions were as follows: (a) anti-mouse, anti-rat and anti-human CXCR4 rabbit polyclonal antibody (ab2074, Abcam, Cambridge, UK), 1:25; (b) anti-human/mouse CXCL12 antibody (MAB350, R&D Systems, Minneapolis, MN, USA), 1:20; (c) anti-mouse, rat and human CD133 rabbit polyclonal antibody (ab19898, Abcam, Cambridge, UK), 1:500. Appropriate positive controls containing the antigens of interest were simultaneously processed. The primary antibody was omitted from negative controls. The tissue sections were washed in water and counterstained with Mayer's hematoxylin. All immunohistochemical analyses were performed in duplicate.

Evaluation of CXCR4, CXCL12, and CD133

Immunoreactivity for CXCR4 was semi-quantified by assessing staining intensity. Cytoplasmic CXCR4 expression was classified as low or high relative to the staining intensity of hepatocytes. Immunoreactivity for CXCL12 was semi-quantified by assessing the staining intensity and ratio (%) of positive cells. CXCL12 expression was scored as 0, no staining; 1, occasional weak staining; 2, moderate staining and 3, intense staining. Positive staining of over 10% of tumor cells was required for scores of 2 and 3 (high expression). CXCL12 expression was classified as low (scores 0 and 1) or high (scores 2 and 3). High-power fields (200×) of 10 random areas within the tumor were evaluated. CD133 immunoreactivity was semi-quantified by assessing the staining intensity and ratios (%) of positively stained cells. CD133 expression was determined as 0, no staining; 1, <5% of tumor cells positively stained and 2, ≥5% of tumor cells positively stained. Amounts of CD133 expression were classified as low (scores 0 and 1) or high (score 2). High-power (200×) fields of 10 random areas within tumors were evaluated. The two investigators (TS and MO) who evaluated the immunohistochemical findings were blinded to the clinicopathological features and prognoses of the patients. The expression of these factors was evaluated both at tumor sites and in hepatocytes.

Table 1 Clinicopathological characteristics of patients with colorectal liver metastases ($n = 92$)

Clinicopathological characteristics	Number of patients
Age	
≥60 years	56
<60 years	36
Gender	
Male	58
Female	34
Lymph node metastasis of the primary lesion	
Positive	58
Negative	34
Timing of metastasis	
Synchronous	44
Metachronous	48
Tumor size	
≥50 mm	26
<50 mm	66
Fibrous pseudo-capsule	
Positive	15
Negative	77
Number of tumors	
Solitary	23
Multiple	69
Primary lesion site	
Colon	53
Rectum	39
Degree of differentiation	
Well, moderately	85
Poorly, mucinous	7

Colorectal cancer cell line and culture medium

The colorectal cancer cell line, SW48 (American Type Culture Collection, Manassas, VA, USA) was cultured in Leibovitz's L-15 (Sigma Aldrich, St. Louis, MO, USA) medium supplemented with 1% penicillin and streptomycin and 10% fetal bovine serum (FBS) [26].

CXCR4 expression determined by fluorescence microscopy

SW48 cells (5×10^5/well in 800 μl) were seeded in four-well slide chambers (LabTek® II Chamber Slide™ System, Nalge Nunc International, Rochester, NY, USA) 24 h and then serum-starved (0.5% FBS) overnight. The cells were stimulated with CXCL12 (200 ng/ml: R&D Systems,) at 37°C for 24 h, fixed in 4% paraformaldehyde at room temperature for 10 min, and then incubated at room temperature for 10 min with 0.3% Triton X-100 and 1.0% bovine serum albumin in PBS. Fixed and permeabilized cells were stained with rabbit anti-human CXCR4 antibody for 60 min at room temperature, followed by anti-rabbit Alexa Fluor® 488 (Invitrogen, Carlsbad, CA, USA) and DAPI (Invitrogen, Carlsbad, CA, USA) for 30 min at room temperature. CXCR4 internalization was then analyzed by fluorescence microscopy.

Statistical analysis

Data were compared using the rank sum test. Associations between discrete variables were assessed using the Fisher exact probability test. Recurrence or death was estimated using the Kaplan–Meier method and statistical significance was examined using the log-rank test. Multivariate analysis was determined using the Cox proportional hazards model. Data were analyzed using SigmaStat 3.0 and SPSS 11.5 software. All data are expressed as means ± SD. Results were considered significant at $P < 0.05$.

Results

CXCR4 expression in metastatic liver tumors

We immunohistochemically examined whether CXCR4 expression in tumors increases in patients with colorectal liver metastases as follows. CXCR4 expression (staining intensity) was compared to that of hepatocytes in specimens of colorectal liver metastases from 92 patients (Fig. 1). The patients were assigned to groups according to the staining intensity of CXCR4 relative to that of hepatocytes. Levels of CXCR4 expression in the cytoplasm of tumor cells were high in 36 (39%) and low in 56 (61%) of the 92 patients. The CXCR4 was also expressed in the nuclei of tumor cells in some patients with colorectal liver metastases. Levels of nuclear CXCR4 expression were high in 23 (25%) and low in 69 (75%) of the 92 patients examined (Fig. 1a, b and c).

CXCR4 expression in metastatic liver tumors and patients' characteristics

We analyzed the characteristics of the patients to determine whether CXCR4 expression in metastatic liver tumors correlates with clinicopathological parameters. Levels of CXCR4 expression in metastatic liver tumors and clinicopathological parameters are shown in Table 2. A fibrous pseudo-capsule defined by HE staining surrounding the tumors of some patients with colorectal liver metastases [24] adversely correlated with high, but not low levels of CXCR4 expression ($P = 0.040$), whereas other clinicopathological parameters did not significantly differ between the two groups (Table 2).

CXCL12 expression in metastatic liver tumors and patient characteristics

We immunohistochemically determined CXCL12 expression in CLM from 92 patients (Fig. 1d, e, and f). Levels of cytoplasmic CXCL12 expression in tumor cells were high in 51 (55%) and low in 41 (45%) of the 92 patients examined, whereas correlations between clinicopathological parameters and CXCL12 expression did not significantly differ between these two groups (Table 2). CXCL12 was also expressed in hepatocytes surrounding the tumors at high and low levels in 68 (74%) and 24 (26%), respectively, of the 92 patients examined (Fig. 1d, e, and f).

Relationship between CXCR4 and CXCL12 expression

Correlations between cytoplasmic CXCL12 and CXCR4 expression in metastatic liver tumors did not significantly differ between the two groups ($P = 0.206$; Table 2). Whereas, the correlations between nuclear CXCR4 expression in tumor cells and CXCL12 expression in hepatocytes significantly differed ($P = 0.030$; Table 2).

Fluorescence microscopy of CXCR4 expression in the SW48 colon cancer cell line

Fluorescence microscopy revealed membrane and cytoplasmic CXCR4 expression in colon cancer cells after 24 h of culture in mock medium (Fig. 2) and increased nuclear expression of CXCR4 after 24 h of exposure to CXCL12. This was confirmed by merged light blue signals of DAPI and Alexa 488 (CXCR4) in nuclei (Fig. 2).

CD133 expression in metastatic liver tumors

An immunohistochemical analysis of tumors revealed high and low CD133 expression in 28 (30%) and 64 (70%) of the 92 patients examined.

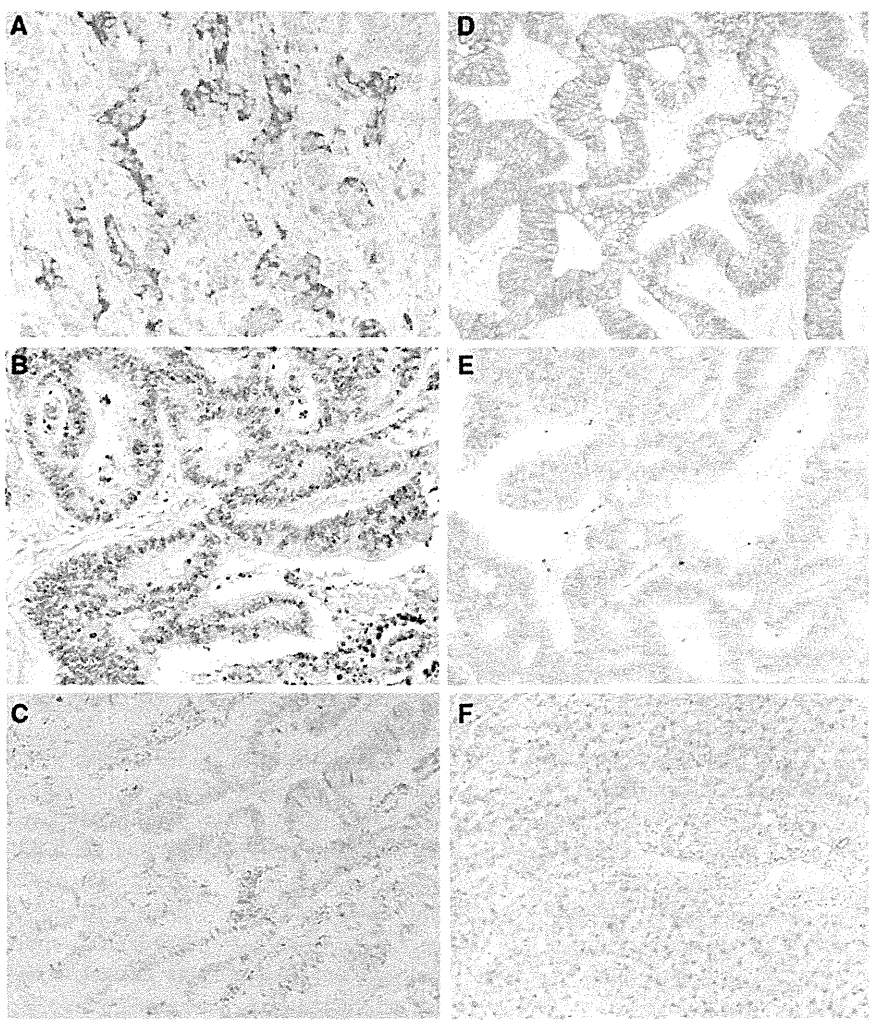

Fig. 1 Immunohistochemical assessment of expression of CXCR4 **a–c** in metastatic liver tumors and of CXCL12 **d–f** in tumors and hepatocytes. **a** Cytoplasmic, **b** nuclear and **c** absent CXCR4 expression. **d** High, **e** low and **f** positive CXCL12 expression in hepatocytes. Original magnification ×200

Table 2 Clinicopathological characteristics are associated with CXCR4 and CXCL12 expression

Clinicopathological characteristics	CXCR4 expression (cytoplasm)			CXCL12 expression		
	High ($n = 36$)	Low ($n = 56$)	P value*	High ($n = 51$)	Low ($n = 41$)	P value*
Age (≥60 years)	26	30	0.084	28	28	0.21
Gender (Male)	22	36	0.83	29	29	0.20
Lymph node metastasis of primary lesion (+)	21	37	0.51	34	24	0.52
Timing of metastasis (synchronous)	18	26	0.83	22	22	0.40
Tumor size (≥50 mm)	11	15	0.81	13	13	0.64
Fibrous capsule (+)	2	13	**0.040**	9	6	0.78
Number of tumors (≥2)	9	14	>0.9	12	11	0.81
Primary lesion site (Colon)	17	36	0.13	30	23	0.83
Degree of differentiation (well, moderately)	33	52	>0.9	47	38	>0.9

CXCL12 expression (Tumor)	CXCR4 expression (tumor)		P value*
	High ($n = 36$)	Low ($n = 56$)	
High ($n = 51$)	23	28	0.206
Low ($n = 41$)	13	28	

CXCL12 expression (Liver)	CXCR4 expression (nucleus)		P value*
	High ($n = 23$)	Low ($n = 69$)	
High ($n = 68$)	21	47	0.030
Low ($n = 24$)	2	22	

*Fisher probability test

Bold values indicate statistically significance

CXCR4 and CXCL12 expression correlated with survival

We analyzed overall survival using the Kaplan–Meier method to determine whether CXCR4 and CXCL12 expression in metastatic liver tumors is related to overall survival after hepatic resection. The results showed a significantly lower overall survival rate in patients with high cytoplasmic and no nuclear CXCR4 expression in tumor cells than in any other groups (Fig. 3a). The overall survival rates were significantly higher in patients with high levels of nuclear CXCR4 expression than in those with none (Fig. 3b), and in those with positive, than negative CXCL12 expression in hepatocytes (Fig. 3c). These rates were significantly lower in patients with positive, than with negative CD133 expression in tumors (Fig. 3d).

We examined whether the CXCR4/CXCL12 expression is a significant prognostic factor for overall and hepatic disease-free survival after hepatic resection using univariate and multivariate analyses. Univariate analysis demonstrated that the number of metastases, primary lymph node involvement, nuclear CXCR4 expression in tumor cells, CXCL12 expression in hepatocytes, and high levels of CD133 expression in tumors were significant prognostic factors for overall survival (Table 3). The number of metastases, tumor size, timing of metastases and CXCL12 expression in hepatocytes were significant prognostic factors for hepatic disease-free survival (Table 3). Multivariate analysis showed that positive primary lymph node involvement, low nuclear CXCR4 expression in tumor cells and low CXCL12 expression in hepatocytes were significant independent prognostic factors for overall survival, and that the timing of metastases, low levels of nuclear CXCR4 expression in tumor cells and low CXCL12 expression in hepatocytes were significant independent prognostic factors for hepatic disease-free survival in patients with colorectal liver metastases (Table 3).

Discussion

This study demonstrated that the expression profiles of CXCR4/CXCL12 correlate with clinical outcomes and might be altered by the tumor microenvironment, thus leading to a change in tumor behavior in CLM. The expression of CXCR4/CXCL12 in terms of chemotactic properties and tumor progression in several malignancies has been described, but expression profiles were analyzed as an intrinsic activity in the tumor environment like that of colorectal carcinoma. In addition, the relationship between

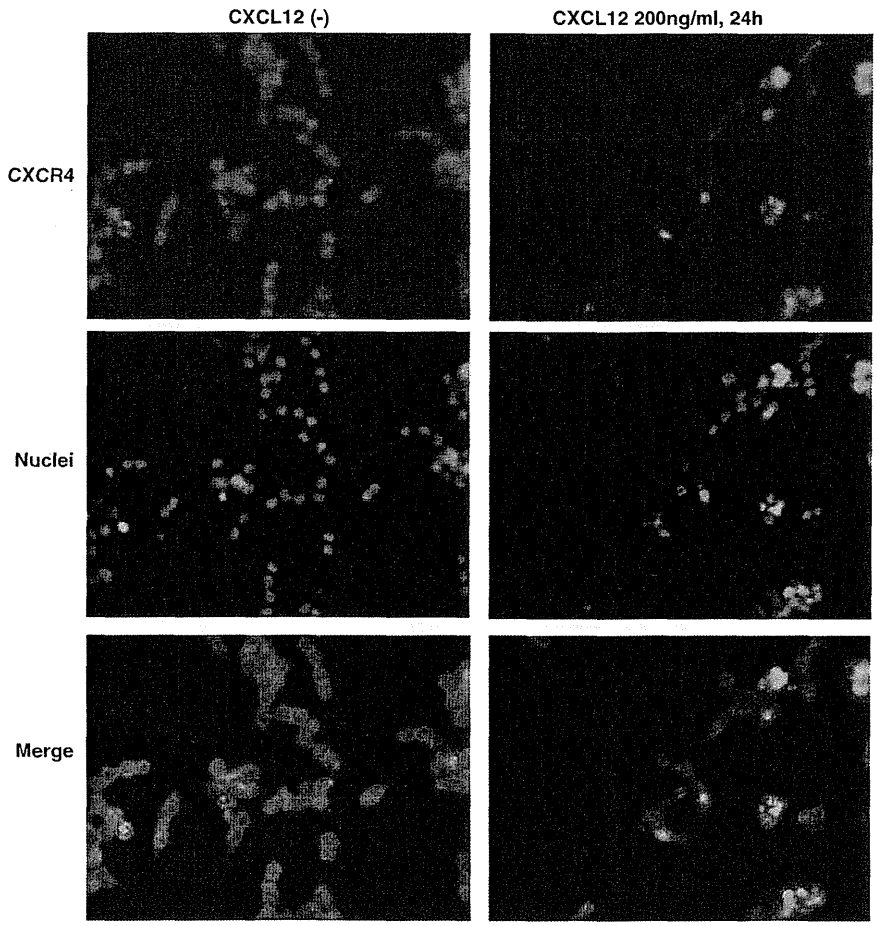

Fig. 2 Nuclear localization of CXCR4 after CXCL12 stimulation in SW48 colon cancer cells. SW48 cells were stimulated with 200 ng/ml CXCL12 for 24 h and then immunostained and observed by fluorescence microscopy. *Green*, membrane and cytoplasmic CXCR4; *deep blue*, nucleus. Some CXCR4 have colocalized in the nucleus (light blue) of stimulated SW48 cells. (Color figure online)

CXCR4/CXCL12 expression and prognosis has not been investigated in a large number of colorectal liver metastases.

The metastatic mechanisms of epithelial-to-mesenchymal transition (EMT) and tumor microenvironment have recently become widely recognized [27]. Chemokines and their receptors were originally identified by the ability to generate chemoattractive interactions between immune cells and sites of inflammation [6]. Recent observations have revealed that cancer cells utilize chemokine networks to modulate the host microenvironment in favor of cancer progression [28]. Several chemokines and their receptors such as CXCR2, CXCR3, CXCR4, CXCR7, CCR2, CCR6, and CCR7 are involved in colorectal cancer [12–15, 29–31]. Interactions between CXCR4 and CXCL12 are considered to play a role in the progression of colon cancer [13, 32]. The EMT is also mediated by the CXCR4/CXCL12 system [33, 34]. These findings suggested that CXCR4 plays a role in tumor progression and metastasis.

Cytoplasmic CXCR4 expression correlates with tumor recurrence and clinical outcomes in several cancers including colon cancer [12, 17, 35]. Circulating cytoplasmic CXCR4-positive tumor cells might be responsible for extravasation and the organ-specific metastasis induced by CXCL12 gradients [29]. The liver is one metastatic site that results from interaction between CXCL12 and CXCR4. The cytoplasmic expression and role of CXCR4 are controversial. The present study found that cytoplasmic CXCR4 expression did not reach statistical difference for poor overall survival and that it did not correlate with CXCL12 expression in metastatic colorectal cancer cells. Therefore, the expression and role of cytoplasmic CXCR4 probably differs between metastatic and primary sites, which would be consistent with the findings of Shim et al. [22].

Some types of cancers express nuclear CXCR4, but its precise function has not been fully elucidated [20, 21, 36–39]. Nuclear CXCR4 expression correlates with a better prognosis in non-small cell lung cancer [20]. Consistent with this finding, nuclear CXCR4 expression closely correlated with better overall and hepatic disease-free survival in the present study. Upregulated nuclear CXCR4 expression might counteract the effect of the cytoplasmic CXCR4 expression that is associated with a poor prognosis. On the other hand, nuclear CXCR4 expression is associated with a poor prognosis in primary colon cancer [21, 38]. Like the

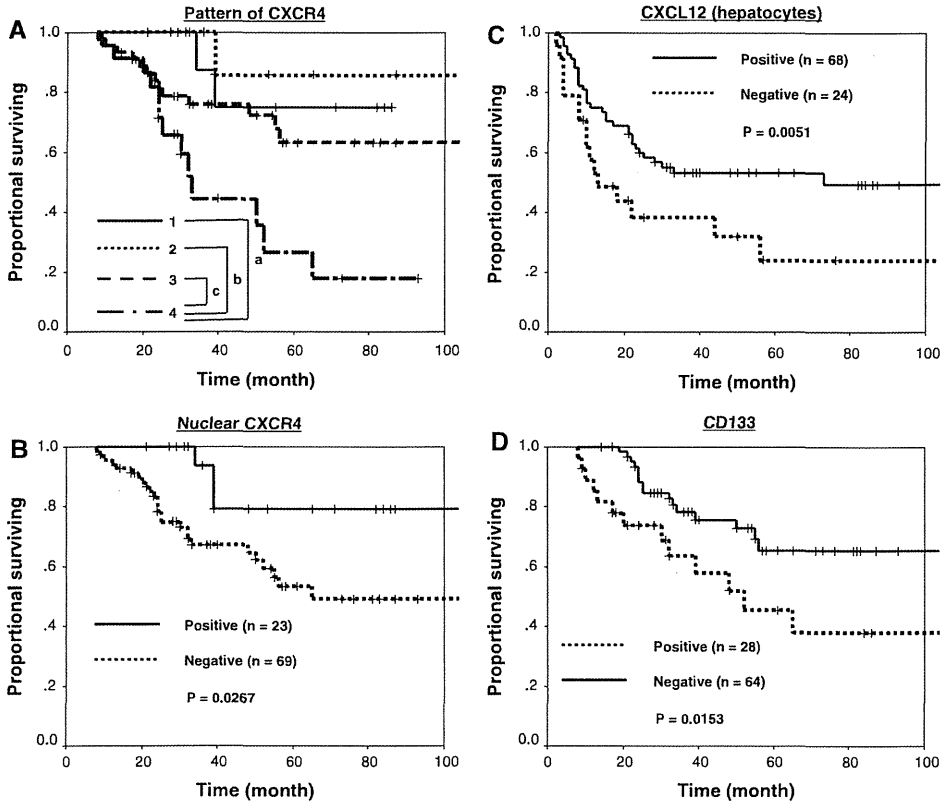

Fig. 3 Overall survival rates stratified by expression of **a** cytoplasmic and nuclear **b** CXCR4. *CY* cytoplasmic expression, *NC* nuclear expression. 1, CY (−) + NC (+); 2, CY (+) + NC (+); 3, CY (−) + NC (−); 4, CY (+) + NC (−). Expression profiles significantly differed (a, $P = 0.0022$; b, $P = 0.0113$; c, $P = 0.0116$). Overall survival rates stratified by expression of **b** nuclear CXCR4, **c** hepatocyte CXCL12, and **d** CD133

role of epidermal growth factor receptor (EGFR) in association with cyclin D1, internalized CXCR4 might act as a transcription factor [38, 40] that could induce tumor progression accompanied by NF-κB activation [41]. However, our data contradict this notion. Although the precise molecular mechanism and role of nuclear CXCR4 expression remain unknown, one theory has been proposed [11, 22, 42–44]. Upregulated CXCL12 in hepatocytes was an independent significant prognosis factor for both overall and hepatic disease-free survival. The results of our fluorescence microscopy study of CXCR4 expression in cancer cell line are consistent with the finding that increased CXCL12 levels cause nuclear CXCR4 internalization in cancer cell lines in vitro [44], and suggest that the tumor microenvironment alters CXCR4 expression profiles in cancer cells. Spano et al. demonstrated that interaction between CXCL12 and CXCR4 might be disrupted when CXCR4 is expressed in the nucleus [20]. Inhibiting CXCR4 and CXCL12 interaction is likely to reduce metastases [45]. These findings suggest that further metastases into organs other than the liver might not be induced by the tumor microenvironment and if so, curative hepatic resection for metastases would improve survival. Nuclear CXCR4 and hepatocyte CXCL12 expression correlated in the current study, suggesting that consistently upregulated CXCL12 expression in the liver alters the microenvironment, reduces cytomembrane CXCR4 expression and leads to CXCR4 internalization. Thus, the tumor microenvironment might be altered in a specific manner after liver metastasis becomes established.

CXCR7 has recently been identified as another receptor for CXCL12 [29]. CXCR4 and CXCL12 expression did not correlate in tumor cells, suggesting that CXCR7 is associated with metastases of colorectal cancer. Although we have no further information about CXCR7 expression, further investigation of interactions between CXCL12 and CXCR7 might be warranted. CXCL12/CXCR4 expression accumulates in CD133 positive tumor cells that might, in part, be derived from cancer stem cells [18, 19]. CD133 expression is an independent prognostic marker of poor survival in colorectal cancer [46]. The present study found that increased CD133 expression tended to indicate poor overall survival, suggesting that that it plays a specific role in the progression of colorectal liver metastases.

Table 3 Univariate and multivariate analysis of predictive factors for overall and hepatic disease-free survival

Factors	Overall survival		Hepatic disease-free survival	
	3-year (MST; months)	*P* value*	3-year (MST; month)	*P* value*
Timing of metastases				
Synchronous ($n = 44$)	65% (65)	0.17	28% (18)	0.0003
Metachronous ($n = 48$)	65%		68%	
Tumor size				
<50 mm ($n = 71$)	76%	0.13	56% (73)	0.0087
≥50 mm ($n = 21$)	67% (52)		26% (17)	
Primary lymph node involvement				
Negative($n = 34$)	89%	0.0128	60%	0.13
Positive ($n = 58$)	66% (56)		43% (24)	
Number of metastases				
≤4 ($n = 74$)	81%	0.0084	55% (73)	0.0044
≥5 ($n = 18$)	48% (32)			
Cytoplasm CXCR4 expression				
Low ($n = 56$)	78%	0.14	51% (56)	0.76
High ($n = 36$)	67%		45% (30)	
Nuclear CXCR4 expression				
Negative ($n = 69$)	67%	0.0267	43% (23)	0.064
Positive ($n = 23$)	93%		68%	
Hepatocyte CXCL12 expression				
Negative ($n = 24$)	49% (25)	0.0051	38% (13)	0.0268
Positive ($n = 68$)	80%		53% (73)	
CD133 expression				
Low ($n = 64$)	78%	0.0153	49% (33)	0.78
High ($n = 28$)	64% (52)		49% (30)	

Factors	95% confidence intervals			
	Relative risk	Lower	Upper	*P* value**
Overall survival				
Timing of metastases (synchronous)	1.27	0.52	3.09	0.60
Tumor size (≥50 mm)	0.94	0.37	2.37	0.89
Primary lymph node involvement (positive)	3.87	1.40	10.7	**0.009**
Number of metastases (≥5)	2.05	0.75	5.59	0.16
Cytoplasm CXCR4 expression (low)	0.43	0.18	1.02	0.056
Nuclear CXCR4 expression (low)	4.05	1.19	13.8	**0.025**
Hepatocyte CXCL12 expression (low)	2.75	1.17	6.55	**0.022**
CD133 expression (high)	2.03	0.94	4.37	0.070
Hepatic disease-free survival				
Timing of metastases (synchronous)	2.54	1.34	4.83	**0.004**
Tumor size (≥50 mm)	1.82	0.92	3.58	0.083
Primary lymph node involvement (positive)	1.73	0.90	3.33	0.099
Number of metastases (≥5)	1.38	0.64	2.98	0.41
Cytoplasm CXCR4 expression (low)	0.89	0.49	1.63	0.71
Nuclear CXCR4 expression (low)	2.40	1.08	5.33	**0.031**
Hepatocyte CXCL12 expression (low)	2.09	1.10	3.98	**0.025**
CD133 expression (high)	1.01	0.53	1.92	>0.9

MST median survival time (months)

* Log-rank test, ** Cox proportional hazards model

Bold values indicate statistically significance

The present study identified a correlation between CXCR4 expression and a fibrous pseudocapsule (FC) surrounding the tumor. According to a previous report, survival is better among patients with, than without FC formation [24]. However, the mechanism for such formation remains obscure. A previous and the present study found a significantly lower microvessel density in patients with, than without FC (data not shown). The tumor environment inside FC might be hypoxic, which would reduce CXCR4 expression [44] and a hypoxic tumor environment beneath FC might further inhibit cytoplasmic CXCR4 expression and tumor progression. Notably, one study has shown that hepatic stellate cells express CXCR4 [47]. Although the mechanism of FC formation has not been clarified, CXCL12 upregulation in the liver probably induces the activation of hepatic stellate cells which produce a fibrotic matrix, thus forming FC.

High levels of nuclear CXCR4 and hepatocyte CXCL12 expression are associated with overall and hepatic disease-free survival compared with other reported clinical factors [23–25]. Thus, the expression profiles of CXCR4 and CXCL12 might predict remnant liver cancer recurrence and a poor prognosis. In conclusion, CXCR4/CXCL12 may play crucial roles in the biologically aggressive behavior of colorectal liver metastasis, and CXCR4 expression in metastatic liver tumors together with CXCL12 upregulation in hepatocytes may be useful to predict the clinical outcomes of patients with CLM after hepatectomy. Further studies are required to define the role of nuclear CXCR4 expression in patients with colorectal liver metastasis.

Acknowledgments This work was supported in part by grants from the Japan Society for the Promotion of Science (Grant# 19591577, 22591500).

References

1. Rosen M, Chan L, Beart RW Jr et al (1998) Follow-up of colorectal cancer: a meta-analysis. Dis Colon Rectum 41:1116–1126
2. Nordlinger B, Guiguet M, Vaillant JC et al (1996) Surgical resection of colorectal carcinoma metastases to the liver. A prognostic scoring system to improve case selection, based on 1568 patients. Association Française de Chirurgie. Cancer 77:1254–1262
3. Fong Y, Cohen AM, Fortner JG et al (1997) Liver resection for colorectal metastases. J Clin Oncol 15:938–946
4. Paget S (1889) The distribution of secondary growth in cancer. Lancet 1:571–573
5. Kakinuma T, Hwang ST (2006) Chemokines, chemokine receptors, and cancer metastasis. J Leukoc Biol 79:639–651
6. Oppenheim JJ, Zachariae CO, Mukaida N et al (1991) Properties of the novel proinflammatory supergene "intercrine" cytokine family. Annu Rev Immunol 9:617–648
7. Murphy PM (2001) Chemokines and the molecular basis of cancer metastasis. N Engl J Med 345:833–835
8. Burger JA, Kipps TJ (2006) CXCR4: a key receptor in the crosstalk between tumor cells and their microenvironment. Blood 107:1761–1767
9. Strieter RM, Burdick MD, Mestas J et al (2006) Cancer CXC chemokine networks and tumour angiogenesis. Eur J Cancer 42:768–778
10. Zlotnik A (2006) Chemokines and cancer. Int J Cancer 119: 2026–2029
11. Koshiba T, Hosotani R, Miyamoto Y et al (2000) Expression of stromal cell-derived factor 1 and CXCR4 ligand receptor system in pancreatic cancer: a possible role for tumor progression. Clin Cancer Res 6:3530–3535
12. Kim J, Mori T, Chen SL et al (2006) Chemokine receptor CXCR4 expression in patients with melanoma and colorectal cancer liver metastases and the association with disease outcome. Ann Surg 244:113–120
13. Schimanski CC, Schwald S, Simiantonaki N et al (2005) Effect of chemokine receptors CXCR4 and CCR7 on the metastatic behavior of human colorectal cancer. Clin Cancer Res 11:1743–1750
14. Ghadjar P, Coupland SE, Na IK et al (2006) Chemokine receptor CCR6 expression level and liver metastases in colorectal cancer. J Clin Oncol 24:1910–1916
15. Yoshidome H, Kohno H, Shida T et al (2009) Significance of monocyte chemoattractant protein-1 in angiogenesis and survival in colorectal liver metastases. Int J Oncol 34:923–930
16. Kollmar O, Rupertus K, Scheuer C et al (2007) Stromal cell-derived factor-1 promotes cell migration and tumor growth of colorectal metastasis. Neoplasia 9:862–870
17. Kim J, Takeuchi H, Lam ST et al (2005) Chemokine receptor CXCR4 expression in colorectal cancer patients increases the risk for recurrence and for poor survival. J Clin Oncol 23:2744–2753
18. Miki J, Furusato B, Li H et al (2007) Identification of putative stem cell markers, CD133 and CXCR4, in hTERT-immortalized primary nonmalignant and malignant tumor-derived human prostate epithelial cell lines and in prostate cancer specimens. Cancer Res 67:3153–3161
19. Lin EH, Hassan M, Li Y et al (2007) Elevated circulating endothelial progenitor marker CD133 messenger RNA levels predict colon cancer recurrence. Cancer 110:534–542
20. Spano JP, Andre F, Morat L et al (2004) Chemokine receptor CXCR4 and early-stage non-small cell lung cancer: pattern of expression and correlation with outcome. Ann Oncol 15:613–617
21. Yoshitake N, Fukui H, Yamagishi H et al (2008) Expression of SDF-1 alpha and nuclear CXCR4 predicts lymph node metastasis in colorectal cancer. Br J Cancer 98:1682–1689
22. Zhang L, Yeger H, Das B et al (2007) Tissue microenvironment modulates CXCR4 expression and tumor metastasis in neuroblastoma. Neoplasia 9:36–46
23. Minagawa M, Makuuchi M, Torzilli G et al (2000) Extension of the frontiers of surgical indications in the treatment of liver metastasis from colorectal cancer: long-term results. Ann Surg 231:487–499
24. Ambiru S, Miyazaki M, Isono T et al (1999) Hepatic resection for colorectal metastases: analysis of prognostic factors. Dis Colon Rectum 42:632–639
25. Fong Y, Fortner J, Sun RL et al (1999) Clinical score for predicting recurrence after hepatic resection for metastatic colorectal cancer: analysis of 1001 consecutive cases. Ann Surg 230: 309–318
26. Hamada K, Monnai M, Kawai K et al (2008) Liver metastasis models of colon cancer for evaluation of drug efficacy using NOD/Shi-scid IL2Rγnull (NOG) mice. Int J Oncol 32:153–159
27. Tse JC, Kalluri R (2007) Mechanisms of metastasis: epithelial-to-mesenchymal transition and contribution of tumor microenvironment. J Cell Biochem 101:816–829

28. Charo IF, Ransohoff RM (2006) The many roles of chemokines and chemokine receptors in inflammation. N Engl J Med 354: 610–621
29. Sun X, Cheng G, Hao M et al (2010) CXCL12/CXCR4/CXCR7 chemokine axis and cancer progression. Cancer Metastasis Rev 29:709–722. Erratum 2011;30:269–270
30. Kawada K, Hosogi H, Sonoshita M et al (2007) Chemokine receptor CXCR3 promotes colon cancer metastasis to lymph nodes. Oncogene 26:4679–4688
31. Speetjens FM, Kuppen PJ, Sandel MH et al (2008) Disrupted expression of CXCL5 in colorectal cancer is associated with rapid tumor formation in rats and poor prognosis in patients. Clin Cancer Res 14:2276–2284
32. Zeelenberg IS, Ruuls-Van Stalle L, Roos E (2003) The chemokine receptor CXCR4 is required for outgrowth of colon carcinoma micrometastases. Cancer Res 63:3833–3839
33. Onoue T, Uchida D, Begum NM et al (2006) Epithelial-mesenchymal transition induced by the stromal cell-derived factor-1/CXCR4 system in oral squamous cell carcinoma cells. Int J Oncol 29:1133–1138
34. Taki M, Higashikawa K, Yoneda S et al (2008) Up-regulation of stromal cell-derived factor-1alpha and its receptor CXCR4 expression accompanied with epithelial-mesenchymal transition in human oral squamous cell carcinoma. Oncol Rep 19:993–998
35. Fukunaga S, Maeda K, Noda E et al (2006) Association between expression of vascular endothelial growth factor C, chemokine receptor CXCR4 and lymph node metastasis in colorectal cancer. Oncology 71:204–211
36. Woo SU, Bae JW, Kim CH et al (2008) A significant correlation between nuclear CXCR4 expression and axillary lymph node metastasis in hormonal receptor negative breast cancer. Ann Surg Oncol 15:281–285
37. Su L, Zhang J, Xu H et al (2005) Differential expression of CXCR4 is associated with the metastatic potential of human non-small cell lung cancer cells. Clin Cancer Res 11:8273–8280
38. Speetjens FM, Liefers GJ, Korbee CJ et al (2009) Nuclear localization of CXCR4 determines prognosis for colorectal cancer patients. Cancer Microenviron 2:1–7
39. Na IK, Scheibenbogen C, Adam C et al (2008) Nuclear expression of CXCR4 in tumor cells of non-small cell lung cancer is correlated with lymph node metastasis. Hum Pathol 39:1751–1755
40. Lin SY, Makino K, Xia W et al (2001) Nuclear localization of EGF receptor and its potential new role as a transcription factor. Nat Cell Biol 3:802–808
41. Huang YC, Hsiao YC, Chen YJ et al (2007) Stromal cell-derived factor-1 enhances motility and integrin up-regulation through CXCR4, ERK and NF-kappaB-dependent pathway in human lung cancer cells. Biochem Pharmacol 74:1702–1712
42. Burger M, Glodek A, Hartmann T et al (2003) Functional expression of CXCR4 (CD184) on small-cell lung cancer cells mediates migration, integrin activation, and adhesion to stromal cells. Oncogene 22:8093–8101
43. Futahashi Y, Komano J, Urano E et al (2007) Separate elements are required for ligand-dependent and -independent internalization of metastatic potentiator CXCR4. Cancer Sci 98:373–379
44. Shim H, Lau SK, Devi S et al (2006) Lower expression of CXCR4 in lymph node metastases than in primary breast cancers: potential regulation by ligand-dependent degradation and HIF-1alpha. Biochem Biophys Res Commun 346:252–258
45. Kim SY, Lee CH, Midura BV et al (2008) Inhibition of the CXCR4/CXCL12 chemokine pathway reduces the development of murine pulmonary metastases. Clin Exp Metastasis 25:201–211
46. Horst D, Kriegl L, Engel J et al (2008) CD133 expression is an independent prognostic marker for low survival in colorectal cancer. Br J Cancer 99:1285–1289
47. Hong F, Tuyama A, Lee TF et al (2009) Hepatic stellate cells express functional CXCR4: role in stromal cell-derived factor-1alpha-mediated stellate cell activation. Hepatology 49:2055–2067

LIVER, PANCREAS, AND BILIARY TRACT

Use of F-18 Fluorodeoxyglucose Positron Emission Tomography With Dual-Phase Imaging to Identify Intraductal Papillary Mucinous Neoplasm

MASAYOSHI SAITO,* TAKESHI ISHIHARA,* MOTOHISA TADA,* TOSHIO TSUYUGUCHI,* RINTARO MIKATA,* YUJI SAKAI,* KATSUNOBU TAWADA,* HARUTOSHI SUGIYAMA,* JO KUROSAWA,* MASAYUKI OTSUKA,‡ YOSHITAKA UCHIDA,§ KATSUHIRO UCHIYAMA,§ MASARU MIYAZAKI,‡ and OSAMU YOKOSUKA*

*Department of Medicine and Clinical Oncology, and ‡Department of General Surgery, Graduate School of Medicine, Chiba University; and §PET Diagnostic Imaging Center, Sannou Hospital Medical Center, Chiba, Japan

BACKGROUND & AIMS: We investigated the usefulness of dual-phase F-18 fluorodeoxyglucose positron emission tomography with computed tomography (FDG-PET/CT) to differentiate benign from malignant intraductal papillary mucinous neoplasms (IPMNs) and to evaluate branch-duct IPMNs. **METHODS:** We used FDG-PET/CT to evaluate IPMNs in 48 consecutive patients who underwent surgical resection from May 2004 to March 2012. IPMNs were classified as benign (n = 16) or malignant (n = 32) on the basis of histology analysis. The ability of FDG-PET/CT to identify branch-duct IPMNs was compared with that of the International Consensus Guidelines. **RESULTS:** The maximum standardized uptake value (SUVmax) was higher for early-phase malignant IPMNs than that for benign IPMNs (3.5 ± 2.2 vs 1.5 ± 0.4, $P < .001$). When the SUVmax cutoff value was set at 2.0, early-phase malignant IPMNs were identified with 88% sensitivity, specificity, and accuracy. The retention index values for malignant and benign IPMNs were 19.6 ± 17.8 and −2.6 ± 12.9, respectively. When the SUVmax cutoff was set to 2.0 and the retention index value to −10.0, early-phase malignant IPMNs were identified with 88% sensitivity, 94% specificity, and 90% accuracy. In identification of branch-duct IPMNs, when the SUVmax cutoff was set to 2.0, the sensitivity, specificity, and accuracy values were 79%, 92%, and 84%, respectively. By using a maximum main pancreatic duct diameter ≥7 mm, the Guidelines identified branch-duct IPMNs with greater specificity than FDG-PET/CT. The Guidelines criteria of maximum cyst size ≥30 mm and the presence of intramural nodules identified branch-duct IPMNs with almost equal sensitivity to FDG-PET/CT. **CONCLUSIONS: Dual-phase FDG-PET/CT is useful for preoperative identification of malignant IPMN and for evaluating branch-duct IPMN.**

Keywords: Imaging; Diagnosis; Comparison; Pancreas; Carcinoma.

Since its first description by Ohashi et al[1] in 1982, the reported incidence of intraductal papillary mucinous neoplasm (IPMN) has been increasing because of improvements in imaging modalities and growing clinical awareness. IPMN is defined as an intraductal tumor formed of papillary proliferations of pancreatic mucin-producing epithelial cells.[2] IPMN manifests in a variety of histologic grades, is associated with the adenoma-carcinoma sequence, and may be benign or malignant.[3] The frequency of malignancy differs according to type of IPMN. The risk of malignancy in main-duct type IPMN is 57%–92%,[4–6] as compared with branch-duct type IPMN, in which the risk of malignancy ranges from 6% to 46%.[7–9] Because of the poor prognosis of invasive carcinoma,[10] tumor resection is the only curative treatment for malignant IPMN. However, preoperative determination of malignant IPMN remains difficult, even with different imaging techniques.

In 2004, the International Association of Pancreatology outlined International Consensus Guidelines (ICG) for the management of IPMN.[11] The ICG recommends surgical resection in all cases of main-duct type IPMN. Because of the low malignant potential of branch-duct type IPMN, the ICG recommends surgical resection in the presence of 1 or more of the following clinical indicators: (1) cyst-related symptoms, (2) main pancreatic duct (MPD) diameter ≥7 mm, (3) cyst size ≥30 mm, (4) presence of intramural nodules, and (5) cyst fluid cytology suspicious/positive for malignancy. However, proper treatment strategy for branch type IPMN has not been well established.

Characterization of IPMN is accomplished by using several imaging modalities such as multidetector row computed tomography, magnetic resonance cholangiopancreatography (MRCP), and endoscopic ultrasonography (EUS). F-18 fluorodeoxyglucose positron emission tomography/computed tomography (FDG-PET/CT) has been widely used in the evaluation of various malignancies. FDG-PET/CT is a functional and anatomic imaging modality that detects abnormalities in glucose metabolism by using a glucose analogue combined with anatomic correlation. However, use of FDG-PET/CT in the evaluation of malignant IPMN has been limited.[12–15] Because FDG is not a tumor-specific substance, it accumulates in inflammatory lesions, which can cause false-positive results.[16] To solve this problem, some investigators[17–19] performed dual-phase FDG-PET imaging, which includes delayed-phase imaging to differentiate benign from malignant lesions in various cancers. However, the useful-

Abbreviations used in this paper: EUS, endoscopic ultrasonography; FDG-PET/CT, F-18 fluorodeoxyglucose positron emission tomography/computed tomography; HGD, high-grade dysplasia; ICG, International Consensus Guidelines; IGD, intermediate-grade dysplasia; IPMN, intraductal papillary mucinous neoplasm; LGD, low-grade dysplasia; MPD, main pancreatic duct; MRCP, magnetic resonance cholangiopancreatography; RI, retention index; SUVmax, maximum standardized uptake value.

1542-3565/$36.00
http://dx.doi.org/10.1016/j.cgh.2012.10.037

ness of dual-phase imaging in differentiating between benign and malignant IPMNs has not been previously examined.

The primary objective of the current study was to evaluate the usefulness of FDG-PET/CT in differentiating between histologically confirmed benign and malignant IPMNs. The efficacy of dual-phase imaging was also examined. In addition, the usefulness of FDG-PET/CT in branch-duct type IPMN was compared with evaluation that is based on clinical features that indicate malignant potential according to the ICG.

Materials and Methods

Patients

Between May 2004 and March 2012, FDG-PET/CT was used in the evaluation of 48 consecutive patients with IPMN in whom tumors were surgically resected at our institute. Final pathologic diagnoses were obtained by pathologic review of the surgical specimens and confirmed on the basis of the World Health Organization classification.[20] In this study, medical records of these 48 histologically confirmed cases of IPMN were analyzed retrospectively.

In all patients, sex, age, serum carcinoembryonic antigen levels, serum carbohydrate antigen 19-9 levels, tumor location, type of IPMN, MPD diameter, cyst size, presence and height of intramural nodules, and maximum standardized uptake value (SUVmax) in the early phase were investigated. In 18 patients, SUVmax in the delayed phase was also investigated. Multidetector row computed tomography, EUS, and MRCP were performed for all patients. In 41 patients, pancreatic juice was sampled before surgical resection for cytologic examination. Diagnoses based on cytology were categorized into the following 5 groups: benign, reactive process, atypical cells indeterminate for malignancy, malignancy strongly suspected, and cytology conclusive for malignancy. Cytologic results in which malignancy was strongly suspected or conclusive were regarded as cancer positive, and atypical results were regarded as cancer negative. In this study, MPD diameter, cyst size, and presence and height of intramural nodules were measured by EUS. IPMN was classified into 2 types, main-duct type and branch-duct type, according to the location of the main lesion and on the basis of histologic features.

Surgical Indications

Surgical resection was performed in all cases of main-duct type IPMN and in cases of branch-duct type IPMN that met at least 1 of the following ICG criteria[11]: cyst size ≥30 mm, MPD diameter ≥7 mm, presence of intramural nodules, or cytologically confirmed malignant and symptomatic IPMN. Types of surgery performed included pancreaticoduodenectomy (n = 23), distal pancreatectomy (n = 23), and pancreatectomy (n = 2).

Histopathologic Diagnosis

According to the World Health Organization classification,[20] IPMN was classified into low-grade dysplasia (LGD), intermediate-grade dysplasia (IGD), high-grade dysplasia (HGD), or invasive carcinoma. In this study, malignant IPMN was defined as HGD and invasive carcinoma, and benign IPMN was defined as LGD and IGD. Histopathologic analysis led to diagnoses of LGD in 14 patients, IGD in 2 patients, HGD in 17 patients, and invasive carcinoma in 15 patients.

F-18 Fluorodeoxyglucose Positron Emission Tomography/Computed Tomography Imaging

FDG-PET/CT was performed in Chiba University Hospital and Sannou Hospital. The PET scanners used were Aquiduo (Toshiba Medical Systems, Tokyo, Japan), Advance NXi (GE Healthcare, Waukesha, WI), and Discovery ST (GE Healthcare). All patients fasted for at least 5 hours before examination. Blood glucose was measured before injection of FDG. The injection dose was 4 MBq/kg depending on the patient's weight. Early-phase scans were performed 60 minutes after injection in all 48 patients. Dual-phase FDG-PET/CT scans were performed in the patients enrolled after April 2009. Delayed-phase scans were performed 120 minutes after injection in 18 patients. The reconstructed images were interpreted by physicians with many years of experience in nuclear medicine. FDG uptake was evaluated both visually and semiquantitatively by using SUVmax. SUVmax was defined as the highest pixel value related to the neoplasm burden in each study. It was computed by using the following formula: SUVmax = Maximum activity concentration in the neoplasm (kBq/mL)/[Injected dose (MBq)/Body weight (kg)]. The retention index (RI) was also defined by using the following formula: $(SUV_{delayed} - SUV_{early}) \times 100/SUV_{early}$.

Statistical Analysis

Statistical differences between subgroups were determined by using the Mann-Whitney U test and the χ^2 test. The optimal cutoff value of SUVmax to differentiate benign from malignant IPMNs was determined by receiver operating characteristic analysis. Sensitivity, specificity, and accuracy were also calculated. All statistical analyses were performed by using SPSS software (SPSS version 20.0; SPSS, Inc, Chicago, IL). P values $<.05$ were considered to be statistically significant.

Results

Clinical characteristics of the 48 patients (32 men, 16 women; mean age, 68.6 ± 7.3 years; range, 51-82 years) included in this study are summarized in Table 1. On the basis of histopathologic analysis, benign IPMN was diagnosed in 16 patients and malignant IPMN in 32 patients.

The significant differences between benign and malignant IPMN cases are summarized in Table 1. No significant differences in sex, age, tumor location, tumor type, tumor markers, cyst size, or presence of intramural nodules were observed between the 2 groups. The mean MPD diameter in malignant IPMN cases was larger than that in benign IPMN cases (8.1 ± 4.0 mm vs 4.7 ± 2.2 mm, $P = .001$). The mean height of the intramural nodules was larger in malignant IPMN cases than that in benign IPMN cases (12.6 ± 6.2 mm vs 7.3 ± 4.7 mm, $P = .021$). In 41 patients, endoscopic retrograde cholangiopancreatography was performed for cytologic analysis of pancreatic juice before surgical resection. From these results, 8 patients (16.7%) were diagnosed with malignant IPMN.

The mean SUVmax in the early phase of IPMN in all 48 cases was 2.9 ± 2.0 (range, 1.0-12.3). The mean SUVmax in the early phase of malignant IPMN was significantly higher than that in benign IPMN cases (3.5 ± 2.2 vs 1.5 ± 0.4, $P < .001$).

Figure 1 depicts correlations between histopathologic types of IPMN and SUVmax in the early phase. Mean SUVmax in the early phase of LGD and IGD, HGD, and invasive carcinoma

Table 1. Clinical Characteristics of 48 IPMN Patients

	Benign (n = 16)	Malignant (n = 32)	*P* value
Sex			.588[a]
Male	12	20	
Female	4	12	
Age (*y*)	67.2 ± 7.9	69.3 ± 7.0	.424[b]
Location			.919[a]
Head	7	16	
Body + tail	9	16	
Type			.234[a]
Main duct	3	13	
Branch duct	13	19	
Diameter of MPD (*mm*)	4.7 ± 2.2	8.1 ± 4.0	.001[b]
Cyst size (*mm*)	27.3 ± 7.6	29.9 ± 20.4	.974[b]
Intramural nodules			.421[a]
Present	10	25	
Absent	6	7	
Height of intramural nodules (*mm*)	7.3 ± 4.7	12.6 ± 6.2	.021[b]
Cytology of pancreatic juice (N = 41)			.466[a]
Negative	11	22	
Positive	1	7	
Tumor marker			
Carcinoembryonic antigen (*ng/mL*)	3.4 ± 1.8	4.0 ± 3.3	.678[b]
Carbohydrate antigen 19-9 (*U/mL*)	16.6 ± 16.6	43.0 ± 60.3	.167[b]
SUVmax (early phase)	1.5 ± 0.4	3.5 ± 2.2	<.001[b]

[a]χ^2 test.
[b]Mann–Whitney *U* test.

were 1.5 ± 0.4, 2.6 ± 0.9, and 4.6 ± 2.7, respectively. The mean SUVmax in the early phase of HGD cases was significantly higher than that of LGD and IGD ($P < .001$). The mean SUVmax in the early phase of invasive carcinoma was also higher than that in HGD cases ($P < .001$).

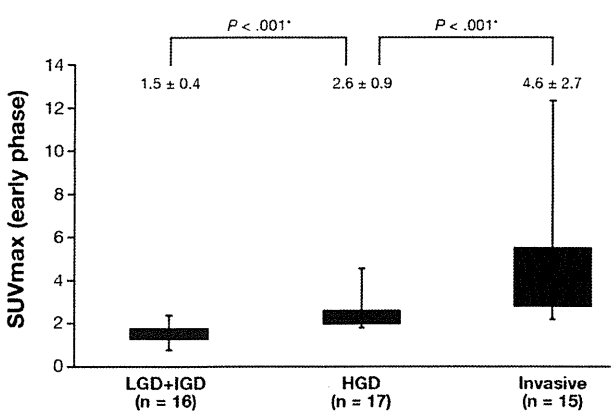

Figure 1. Correlation between pathologic type IPMN and SUVmax in the early phase. The SUVmax on early phase of LGD and IGD, HGD, and invasive carcinoma was 1.5 ± 0.4, 2.6 ± 0.9, and 4.6 ± 2.7, respectively. The SUVmax of HGD was statistically higher than those of LGD and IGD ($P < .001$). The SUVmax of invasive carcinoma was also higher than that of HGD ($P < .001$). *Mann–Whitney *U* test.

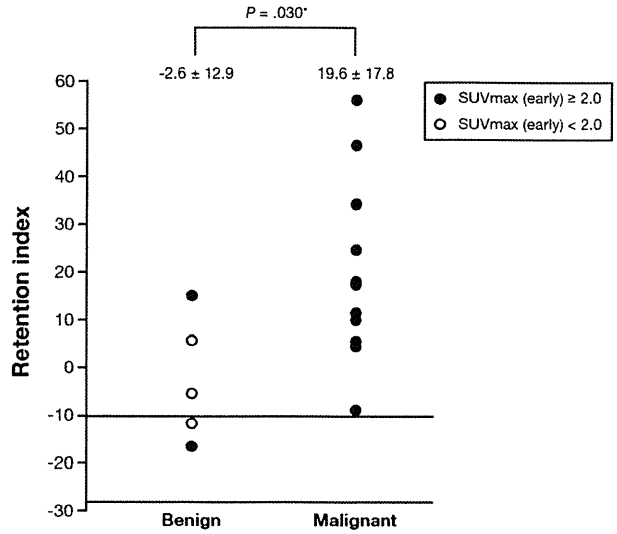

Figure 2. Results for 18 patients in whom dual-phase FDG-PET/CT was performed. Twelve of 13 malignant IPMNs (92.3%) had further increase in SUVmax; 3 of 5 benign IPMNs (60.0%) had decrease in SUVmax on delayed phase. The RI of malignant and benign IPMNs was 19.6 ± 17.8 and −2.6 ± 12.9 ($P = .030$). If a combination of the SUVmax cutoff value of 2.0 in the early phase and the RI value of −10.0 for detection of malignant IPMN was used, one false-positive adenoma case (SUVmax: early 2.4, delayed 2.0) may be diagnosed as benign IPMN. *Mann–Whitney *U* test.

In this study, dual-phase FDG-PET/CT was performed in 18 patients. Histopathologic analysis identified LGD and IGD in 5 of these patients, HGD in 4, and invasive carcinoma in 9. Figure 2 shows RI values for these 18 patients. In 12 of the 13 cases of malignant IPMN (92.3%), SUVmax increased further in the delayed phase, whereas in 3 of 5 cases of benign IPMN (60.0%), SUVmax decreased in the delayed phase. RI values in malignant and benign IPMNs were 19.6 ± 17.8 and −2.6 ± 12.9, respectively. Differences between the 2 groups were statistically significant ($P = .030$).

Table 2 displays values for the sensitivity, specificity, and accuracy of FDG-PET/CT from the receiver operating characteristic analysis of malignant IPMN cases. When the cutoff value of SUVmax in the early phase was set to 2.0, the sensitivity, specificity, and accuracy in malignant IPMN cases were all 88%. When the cutoff value of SUVmax in the early phase was set to 2.0 and the RI value was set at −10.0, the sensitivity, specificity, and accuracy of FDG-PET/CT in malignant IPMN cases improved to 88%, 94%, and 90%, respectively.

The usefulness of FDG-PET/CT in evaluation of branch-duct type IPMN was compared with that of evaluation according to the clinical features indicating malignant potential in IPMN, as outlined by the ICG (Table 3). In cases with branch-duct type IPMN, when the cutoff value of SUVmax in the early phase was set to 2.0, the sensitivity, specificity, and accuracy of FDG-PET/CT in identifying malignant IPMN cases were 79%, 92%, and 84%, respectively. By using the criteria of maximum MPD diameter ≥7 mm and cytologic analysis of pancreatic juice, specificity was superior to that of FDG-PET/CT, but sensitivity and accuracy were inferior to those of FDG-PET/CT. On the other hand, by using the criteria of maximum cyst size ≥30 mm and the presence of intramural nodules, sensitivity

Table 2. Diagnosis by Using SUVmax (Early Phase) Alone and Combination of SUVmax (Early Phase) and RI for Detection of Malignant IPMNs

	Final diagnosis		
	Benign	Malignant	
FDG-PET/CT dizagnosis	LGD + IGD	HGD	Invasive
Cutoff value: 2.0 for SUVmax in early phase			
Positive	2	13	15
Negative	14	4	0
Sensitivity (%)			88
Specificity (%)			88
Accuracy (%)			88
Cutoff value: 2.0 for SUVmax in early phase and −10.0 for RI			
Positive	1	13	15
Negative	15	4	0
Sensitivity (%)			88
Specificity (%)			94
Accuracy (%)			90

was almost equal to that of FDG-PET/CT, but specificity and accuracy were inferior to those of FDG-PET/CT.

Discussion

In this study, the preoperative usefulness of FDG-PET/CT in differentiating between histologically confirmed benign and malignant IPMNs was evaluated. When the cutoff value for SUVmax in the early phase was set to 2.0, the sensitivity, specificity, and accuracy in identifying malignant IPMN cases were all high (88%). Several other studies have also demonstrated the usefulness of FDG-PET/CT in detecting malignant IPMN. Sperti et al[12] reported sensitivity, specificity, and accuracy levels of 92%, 97%, and 95%, respectively, at a cutoff level of 2.5 in 64 patients with IPMN. Tomimaru et al[13] examined several cutoff levels in 29 cases of IPMN. The sensitivity, specificity, and accuracy levels in that study were 93%, 100%, and 96%, respectively, at a cutoff level of 2.5 and 93%, 86%, and 89%, respectively, at a cutoff level of 2.0.

In the current study, the optimal cutoff value was set at 2.0, slightly lower than that used in previous studies. On the basis of the results of this study and those of previous studies, a cutoff value between 2.0 and 2.5 may be optimal. The cutoff value was low in this study because of the higher number of patients diagnosed as HGD than were diagnosed with invasive carcinoma in the group of patients with malignant IPMN. In the report of Sperti et al,[12] 21 of 26 malignant IPMN cases were diagnosed with invasive carcinoma. In the report of Tomimaru et al,[13] 11 of 14 malignant IPMN cases were diagnosed with invasive carcinoma. Therefore, the incidence of invasive carcinoma was higher in those studies than in the present study.

FDG-PET/CT has been widely used in the evaluation of various malignant lesions, but high SUVmax may also be found in various benign conditions evaluated by using this modality because FDG is not a tumor-specific substance. FDG also accumulates in inflammatory lesions, which can cause false-positive results.[16] Dual-phase FDG-PET/CT has been performed in some studies[17-19] to differentiate benign from malignant lesions in various cancers. The longer time required for levels of FDG to plateau in cancer cells than in inflammatory cells may be related to the up-regulation of glucose consumption demonstrated in malignant cells to obtain more energy for proliferation. This leads to graded concentrations of FDG in tumor cells. In contrast, a prolonged period of FDG uptake is less common in inflammatory lesions or normal tissues.[19] Potential limitations of dual-phase FDG-PET/CT include its low availability, high exposure to radiation, and increased procedural time.

Table 3. Usefulness of FDG-PET/CT in Evaluation of Branch-Duct Type IPMN Compared With That of Evaluation According to Clinical Features Indicating Malignant Potential in IPMN, as Outlined by the ICG

	Final diagnosis					
	Benign	Malignant				
Clinical parameters	LGD + IGD	HGD	Invasive	Sensitivity (%)	Specificity (%)	Accuracy (%)
FDG-PET/CT cutoff value: 2.0 for SUVmax in early phase						
Positive	1	8	7	79	92	84
Negative	12	4	0			
Diameter of MPD (*mm*)						
≥7	0	5	4	47	100	69
<7	13	7	3			
Cyst size (*mm*)						
≥30	9	9	6	79	31	59
<30	4	3	1			
Intramural nodules						
Present	8	11	5	84	38	66
Absent	5	1	2			
Cytology of pancreatic juice (N = 26)						
Positive	0	1	1	13	100	46
Negative	10	9	5			

In pancreatic diseases, Nakamoto et al[21] suggested that dual-phase FDG-PET/CT may be a reliable method of differentiating pancreatic cancer from chronic pancreatitis. Okano et al[22] indicated that dual-phase FDG-PET/CT is a useful modality for detection of small pancreatic cancers. However, the usefulness of dual-phase FDG-PET imaging in differentiation between benign and malignant IPMNs was not examined in other studies. IPMN shows a wide spectrum of histologic grades ranging from benign to malignant neoplasms. Benign IPMN is thought to be low in metabolic activity; therefore, we assumed SUVmax of benign IPMN to decrease in the delayed phase.

In this study, dual-phase FDG-PET/CT imaging was performed in 18 patients. RI values in malignant and benign IPMN cases were 19.6 ± 17.8 and −2.6 ± 12.9, respectively, and a significant difference was observed between the 2 groups. Furthermore, in 12 of 13 malignant IPMN cases (92.3%), SUVmax increased further in the delayed phase, whereas in 3 of 5 benign IPMN cases (60.0%), SUVmax decreased in the delayed phase. If a combination of the SUVmax cutoff value of 2.0 in the early phase and the RI value of −10.0 for detection of malignant IPMN was used, one false-positive case of adenoma (SUVmax: early phase 2.4, delayed phase 2.0) may be diagnosed as benign IPMN. Specificity improved from 88% to 94%, and accuracy improved from 88% to 90%. Pancreatitis had been observed 1 month before FDG-PET/CT examination in this false-positive case; therefore, FDG accumulation in an inflammatory lesion may have been responsible for this false-positive finding. Thus, this 2-step method of FDG-PET/CT may be useful for differentiating between benign and malignant IPMNs.

The ICG recommends surgical resection for all cases of main-duct type IPMN. On the other hand, branch-duct type IPMN has low malignant potential. However, management of branch-duct type IPMN has not been well established. In this study, FDG-PET/CT achieved good sensitivity, specificity, and accuracy in branch-duct type IPMN (79%, 92%, and 84%, respectively). FDG-PET/CT was also useful in differentiating between benign and malignant disease in branch-duct type IPMN. The ICG recommends evaluation according to cyst size, MPD diameter, and the presence of intramural nodules in the tumor in determination of malignant potential in cases of IPMN. The validity of these recommendations for the detection of malignancy was retrospectively evaluated in 2 follow-up studies. Both studies found the ICG criteria to have a sensitivity of 100% in diagnosing malignancy. However, the specificity of the guidelines in diagnosing malignancy was only 23%–31%, resulting in a relatively high resection rate for those without malignancy.[23,24]

In this study, the usefulness of FDG-PET/CT in detection of malignancy in branch-duct type IPMN was compared with detection that was based on these clinical features and EUS findings. EUS is a highly operator-dependent procedure, but several retrospective studies[25,26] have demonstrated its accuracy in the diagnosis of IPMN. EUS has been used to detect intramural lesions in the pancreatic duct, with good results. Nakagawa et al[27] found EUS to be highly sensitive for intramural lesion detection in cases of IPMN, but the specificity of this modality was low, as indicated by the relatively high rate of false-positive cases in that study. These results were caused by mucin in the pancreatic duct, which may appear to be intramural lesions on EUS. In the current study, EUS was sufficiently sensitive in determination of cyst size ≥30 mm and the presence of intramural nodules, but specificity and accuracy were inferior to those of FDG-PET/CT. On the other hand, EUS showed good specificity for MPD diameter ≥7 mm, but its sensitivity and accuracy were inferior to those of FDG-PET/CT. These results demonstrate the usefulness of FDG-PET/CT in branch-duct type IPMN compared with an evaluation that was based on clinical features suggesting malignant potential. In the current study, clinical features were measured on the basis of EUS findings, but MRCP also has been reported to be effective for evaluating the ICG criteria.[28] Baiocchi et al[29] suggested that a combination of MRCP and FDG-PET/CT would be optimal for branch-duct IPMN.

Suggestions for treatment strategies in cases of IPMN can be made on the basis of the results of the current study. Operative adaptations have been narrowed down according to the ICG criteria for IPMN; in these patients, if a combination of the SUVmax cutoff value of 2.0 in the early phase and the RI value of −10.0 in the FDG-PET/CT study was used, the diagnostic accuracy may be improved. Further studies on larger numbers of patients are necessary to confirm the reliability of this strategy.

Conclusions

FDG-PET/CT with dual-phase imaging is a useful clinical modality for preoperative determination of malignant IPMN. FDG-PET/CT is useful in the evaluation of branch-duct type IPMN compared with evaluation that is based on the clinical features suggesting malignant potential outlined in the ICG.

References

1. Ohhashi K, Murakami Y, Maruyama M, et al. Four cases of mucus-secreting pancreatic cancer. Prog Dig Endosc 1982;20: 348–351.
2. Kloppel G, Solcia E, Longnecker DS, et al. Histological typing of tumors of the exocrine pancreas. In: World Health Organization: international histological classification of tumours. 2nd ed. Berlin, Germany: Springer, 1996:15–21.
3. Goh BK, Tan YM, Cheow PC, et al. Cystic neoplasms of the pancreas with mucin-production. Eur J Surg Oncol 2005;31:282–287.
4. Salvia R, Fernández-del Castillo C, Bassi C, et al. Main-duct intraductal papillary mucinous neoplasms of the pancreas: clinical predictors of malignancy and long-term survival following resection. Ann Surg 2004;239:678–685.
5. Sugiyama M, Izumisato Y, Abe N, et al. Predictive factors for malignancy in intraductal papillary-mucinous tumours of the pancreas. Br J Surg 2003;90:1244–1249.
6. Terris B, Ponsot P, Paye F, et al. Intraductal papillary mucinous tumors of the pancreas confined to secondary ducts show less aggressive pathologic features as compared with those involving the main pancreatic duct. Am J Surg Pathol 2000;24:1372–1377.
7. Sohn TA, Yeo CJ, Cameron JL, et al. Intraductal papillary mucinous neoplasms of the pancreas: an updated experience. Ann Surg 2004;239:788–797.
8. Kitagawa Y, Unger TA, Taylor S, et al. Mucus is a predictor of better prognosis and survival in patients with intraductal papillary mucinous tumor of the pancreas. J Gastrointest Surg 2003;7: 12–19.
9. Matsumoto T, Aramaki M, Yada K, et al. Optimal management of the branch duct type intraductal papillary mucinous neoplasms of the pancreas. J Clin Gastroenterol 2003;36:261–265.